Wind Direction Retrieval from Rain-contaminated X-band Nautical Radar Images

Yali Wang, *Student Member, IEEE*, Weimin Huang, *Senior Member, IEEE*
Faculty of Engineering and Applied Science, Memorial University of Newfoundland
St John's, NL, Canada, A1B 3X5
yw8366@mun.ca, weimin@mun.ca

***Abstract*—In this paper, an algorithm for retrieving wind direction from rain-contaminated radar images collected under low wind speed conditions is presented. The algorithm investigates radar backscatter in the wavenumber domain and determines wind directions based on spectral components with wavenumbers of [0.01, 0.2]. The algorithm has been tested using rain-contaminated X-band marine radar images and shipborne anemometer data collected on the east coast of Canada. Comparison with the anemometer data shows the root mean square error of wind direction retrieved from rain-contaminated images collected under low wind speeds is reduced by $25.2°$.**

I. INTRODUCTION

Wind direction retrieval from X-band marine radar images has raised wide interest during the past two decades. In 2003, Dankert *et al.* [1], [2] proposed a method to retrieve wind direction from X-band radar images obtained on a fixed platform with wind-induced streaks on integrated radar images. Lund *et al.* [3] presented a curve fitting method to retrieve wind direction from a moving platform in 2012. The method utilized a sinusoidal function to fit averaged radar backscatter according to azimuth directions. Wind direction is determined as the direction corresponding to the peak of the fitted curve. Vicen-Bueno *et al.* [4] proposed a method in which wind direction is determined as the direction of the maximum range distance on integrated radar images. The latter two methods are based on the observation that for a HH-polarized X-band marine radar operating at grazing incidence, radar backscatter has a single peak in the upwind direction [5]-[7].

All the above wind direction retrieval methods have been shown to work effectively. However, they were only applied to rain-free images. Rain influences radar backscatter and alters the dependence of the image intensity on the azimuth. The effect of rain on radar images is not significant under high wind speed conditions, where wind force dominates [8], [9]. However, for rain-contaminated images collected under low wind speeds, rain could enhance radar backscatter and alter surface roughness in most directions (an example is shown in Fig. 1 (a)). Thus, the accuracy of retrieved wind directions from existing methods may drop [10]. In this paper, an algorithm to retrieve wind direction from rain-contaminated radar images collected under low wind speed conditions is proposed.

II. WIND DIRECTION RETRIEVAL METHOD

Different from existing algorithms, the proposed algorithm is based on the analysis of radar backscatter in the wavenumber domain. The radar backscatter samples in each azimuth are Fourier transformed into the wavenumber domain to generate the wavenumber spectrum

$$E_\theta(k) = \sum_{n=0}^{N-1} I_\theta(n) e^{-j\frac{2\pi}{N}kn} \tag{1}$$

where N is the total number of backscatter samples (i.e. image pixel intensities) in one azimuth, $I_\theta(n)$ is nth pixel intensity in azimuth direction θ, $E_\theta(k)$ represents the spectral value of wavenumber k on direction θ. An example of a wavenumber spectrum for one azimuth is shown in Fig. 2. The spectral values with $k > 0$ result from intensity variation and could be a reflection of surface wave signatures.

After performing Fourier transformation to each azimuth, full wavenumber spectra could be obtained according to azimuth directions. Next, a normalization process is implemented by dividing every spectral value with the maximum spectral value of all azimuths in an image. In order to detect surface wave signatures, the spectral points over the wavenumber range [0.01, 0.2], corresponding to waves with wavelengths between 30 m to 628 m, are chosen. An integral of the normalized spectra over the selected wavenumber range is calculated for each azimuth direction. For azimuth direction θ,

$$S_\theta = \int_{0.01}^{0.2} |E_\theta(k)|\, dk \tag{2}$$

where $|E_\theta(k)|$ is the spectral magnitude of wavenumber component k. Then, S_θ is curve-fitted by the same sinusoidal function proposed by Lund *et al.* [3]

$$S_\theta = a_0 + a_1 \cos^2(0.5(\theta - a_2)) \tag{3}$$

where a_0, a_1, a_2 are parameters which could be determined by least-squares fitting. The fitted result for data shown in Fig. 1 (a) is displayed in Fig. 1 (c). Wind direction is determined as the peak of the fitted curve and found to be $254°$, with a difference of $12°$ from the anemometer-measured wind direction. On the other hand, the wind direction retrieved using the curve fitting method in [3] is $87°$ (shown in Fig. 1 (b)). This may be because the radar image in Fig. 1 (a) was significantly

978-0-933957-43-5 ©2015 MTS

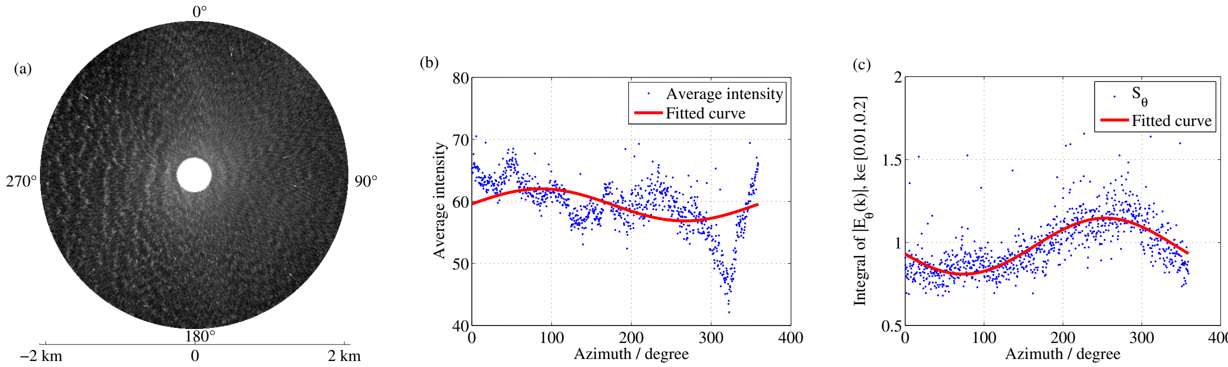

Fig. 1. (a) A rain-contaminated image collected under low wind speed conditions (obtained on 05:24, Nov. 27, 2008), wind direction measured by anemometers: $266°$; (b) Curve fitting result using the method in [3] (the retrieved wind direction is $87°$); (c) Curve fitting result using the proposed method (the retrieved wind direction is $254°$).

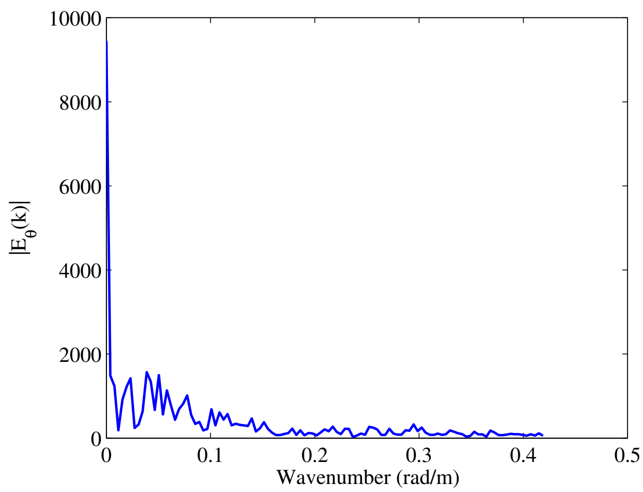

Fig. 2. Wavenumber spectrum of data in one azimuth

affected by rain and the dependence of backscatter intensity on wind direction has been altered.

III. Results

A. Data Overview

The algorithm was tested with the radar data provided by Defence Research and Development Canada (DRDC). The experiments were conducted on the Canadian Navy research ship CFAV Quest from Nov. 26, 2008 to Nov. 29, 2008. The location of the experiment was about 220 km from the coast of Halifax ($42°30'$ N, $62°5'$ W), with a water depth of about 200 m. A 9.41 GHz HH-polarized radar and two anemometers were installed on the ship. The sampling frequency of the radar was 20 MHz. Data was recorded for the range of 240 m to 2160 m from the radar, with a range resolution of 7.5 m. To obtain better accuracy, data utilized for low-wind-speed rain cases were in the range of 540-2160 m. The radar was connected to the Wave Monitoring System (WaMoS II) [11]. This system digitized radar backscatter into 8-bit binary numbers, corresponding to image intensity from 0 to 255. The radar collected one image every two seconds.

B. Low-wind-speed Rain-contaminated Image Recognition

Rain-contaminated images could be identified based on zero pixel percentage (ZPP) [3]. Here, ZPP is defined as the percentage of image pixels with intensities below 5 to the overall pixel number. If the ZPP of an image is smaller than 10%, such an image will be regarded as a rain-contaminated image [12]. However, the identified rain-contaminated radar images contain data collected under low wind speeds as well as high wind speeds. In order to distinguish the rain-contaminated images collected under low wind speeds from those under high wind speeds, a parameter called high pixel percentage (HPP) i.e., the ratio of pixels with intensity higher than 100 to the overall pixel number, is defined. If the HPP of a rain-contaminated image is lower than 15%, the image will be identified as a low-wind-speed rain case.

The ZPP and HPP results are shown in Fig. 3 (b). It could be found that data in four periods (4861 images in total) are identified as low-wind-speed rain cases. These results coincide with the anemometer-measured wind speeds (see Fig. 4 (a)) and rain gauge-measured rain rates (see Fig. 4 (b)).

C. Wind Direction Retrieval Results

Both the curve fitting method in [3] and the proposed method were applied to the low-wind-speed rain-contaminated images selected by ZPP and HPP. The averaged wind directions of the two anemometers were utilized as the reference for comparison with the radar results. The retrieved wind directions were averaged every ten minutes and shown in Fig. 3 (a). It was found that for rain-contaminated images collected under low wind speed conditions, the root mean square error of wind direction derived using the curve fitting method in [3] is $46.7°$. On the other hand, the root mean square error of wind direction retrieved using the proposed method is $21.6°$. The wind direction retrieval accuracy for low wind speed rain cases is improved by $25.1°$ with the proposed method.

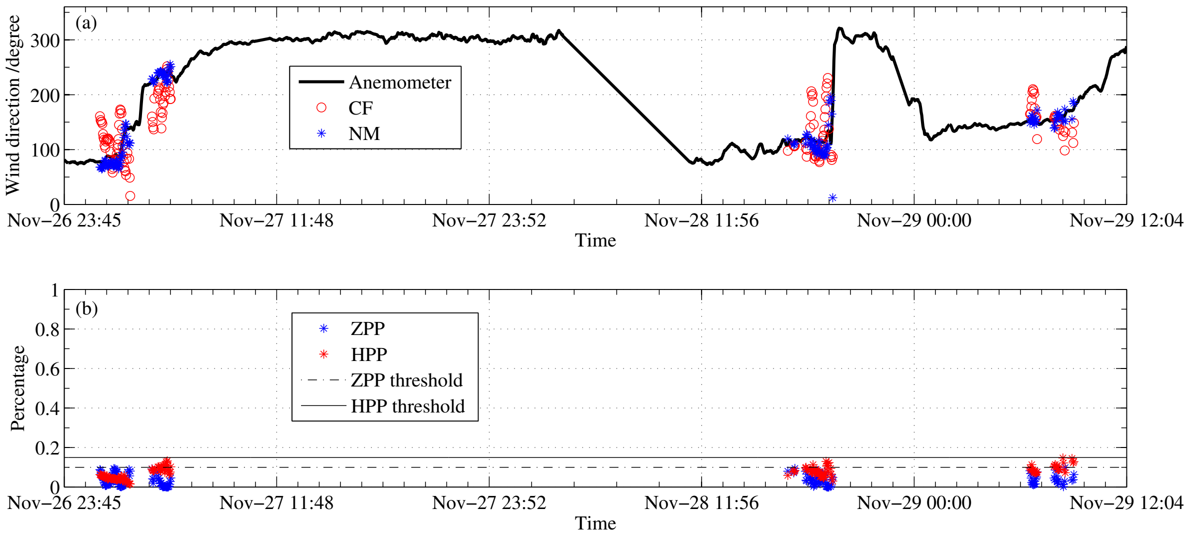

Fig. 3. Results: (a) retrieved wind directions, the root mean square error for Curve Fitting method (CF): $46.7°$, the root mean square error for the new method (NM): $21.6°$; (b) Zero Pixel Percentage (ZPP) and High Pixel Percentage (HPP).

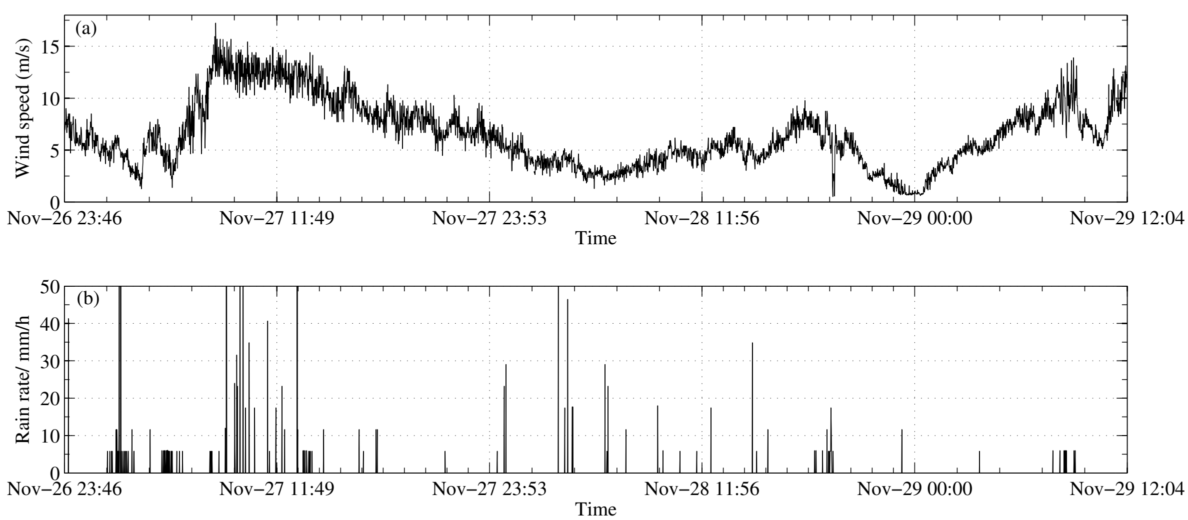

Fig. 4. (a) Measured wind speeds; (b) Measured rain rates.

IV. Conclusion

A method for retrieving wind direction from rain-contaminated X-band marine radar images collected under low wind speed conditions has been presented. The method is designed based on analysis in the wavenumber domain. Wind direction is retrieved based on the spectral points corresponding to wavenumbers in the range of [0.01, 0.2]. Comparison with the curve fitting method in [3] shows that the root mean square error of wind direction retrieved from rain-contaminated data associated with low wind speeds is reduced by $25.1°$ with the proposed method.

In the future, a method for improving wind speed retrieval from rain-contaminated radar images needs to be developed.

Acknowledgements

The authors would like to thank Dr. E. Thornhill of Defence Research and Development Canada for providing radar and anemometer data. This work was supported in part by Natural Sciences and Engineering Research Council of Canada Discovery Grant (NSERC 402313-2012) and the Memorial University Seed, Bridge and Multidisciplinary Grant (20151381) to Dr. Weimin Huang.

REFERENCES

[1] H. Dankert, J. Horstmann, and W. Rosenthal, "Ocean wind fields retrieved from radar-image sequences," *J. Geophys. Res.: Oceans*, vol. 108, no. C11, pp. 16-1-16-11, Nov. 2003.

[2] H. Dankert and J. Horstmann, "A marine radar wind sensor," *J. Atmos. Ocean. Technol.*, vol. 24, no. 9, pp. 1629-1642, Sep. 2007.

[3] B. Lund, H. C. Graber, and R. Romeiser, "Wind retrieval from shipborne nautical X-band radar data," *IEEE Trans. Geosci. Remote Sens.*, vol. 50, no. 10, pp. 3800-3811, Oct. 2012.

[4] R. Vicen-Bueno, J. Horstmann, E. Terril, T. De Paolo, and J. Dannenberg, "Real-time ocean wind vector retrieval from marine radar image sequences acquired at grazing angles," *J. Atmos. Ocean. Technol.*, vol. 30, no. 1, pp. 127-139, Jan. 2013.

[5] P. H. Y. Lee, J. D. Barter, K. L. Beach, C. L. Hindman, B. M. Lake, H. Rungaldier, J. C. Shelton, A. B. Williams, R. Yee, and H. C. Yuen, "X-band microwave backscattering from ocean waves," *J. Geophys. Res.*, vol. 100, no. C2, pp. 2591-2611, Feb. 1995.

[6] D. B. Trizna and D. J. Carlson, "Studies of dual polarized low grazing angle radar sea scatter in nearshore regions," *IEEE Trans. Geosci. Remote Sens.*, vol. 34, no. 3, pp. 747-757, May 1996.

[7] H. Hatten, F. Ziemer, J. Seemann, and J. Nieto-Borge, "Correlation between the spectral background noise of a nautical radar and the wind vector," in *Proc. 17th Int. Conf. Offshore Mech. Arctic Eng. (OMAE)*, Lisbon, Portugal, Jun. 1998.

[8] Z. Yang, S. Tang and J. Wu, "An experimental study of rain effects on fine structures of wind waves," *J. Phys. Oceanogr.*, vol. 27, no. 3, pp. 419-130, 1997.

[9] R. K. Moore, Y. S. Yu, A. K. Fung, D. Kaneko, G. J. Dome, and R. E. Werp, "Preliminary study of rain effects on radar scattering from water surfaces," *IEEE J. Oceanic Eng.*, vol. 4, pp. 31-32, 1979.

[10] Y. Liu, W. Huang, and E. W. Gill, "Analysis of the effects of rain on surface wind retrieval from X-band marine radar images," *Oceans' 14 MTS/IEEE*, St. John' s, Canada, 2014.

[11] (2012, May). WaMoS II Wave and surface current monitoring system operating manual version 4.0. [Online]. Available: oceanwaves.org.

[12] Y. Liu, W. Huang and E. W. Gill, "Comparison of algorithms for wind parameters extraction from shipborne X-band marine radar images," *IEEE J. Sel. Topics Appl. Earth Observ. Remote Sens.*, vol. 8, no. 2, pp. 896-906, 2015.